International Journal of
INTELLIGENT SYSTEMS AND APPLICATIONS IN ENGINEERING
ISSN:2147-6799 www.ijisae.org Original Research Paper

Heuristic Algorithms for Power Quality Analysis in IEEE-33 & IEEE-57 Bus Systems Using Fact Devices and Tracking

K. Swarna Latha[1], Dr. P. Mallikarjuna Sharma[2], Prof. M. Manjula[3]

Submitted: 05/05/2024 **Revised**: 18/06/2024 **Accepted**: 25/06/2024

Abstract: DGs have become increasingly important to the grid in connection with renewable energy systems as fossil fuels run out and pollution is on the rise. The integration of renewable energy sources into low- and medium-voltage distribution networks has opened up a new field of study. To ensure that distributed generation (DG) connections to the grid meet power quality standards, electronic power converters are a common component of renewable energy systems. In this case, major power quality issues will always occur if the inverters' switching frequencies are not appropriately location. On the other hand, power quality reductions can cause acute problems in power networks, such as decreased performance, decreased useful life and efficiency of electrical and electronic equipment in the network, and series and parallel resonance caused by inductors and capacitors in some harmonics, which corrupts the distribution voltage. The present work focuses on quality assurance with compensation using nature inspired algorithms with DG placement after tracking. It compensates by adding fact devices. MBO, GWO and Cuckoo search algorithms are used in the present research and devices like DVR and Dstat.Com are added along with DG. The quality parameters are compared with the existing and in order to increase the robustness hybrid algorithms with any two are suggested.

Keywords: *DG, Heuristic algorithms, Power quality, Tracking, Facts, Harmonics*

1. Introduction:

As renewable energy sources become more widespread, the need for reliable and secure distribution networks has become increasingly important. This has caused a major surge in research and development into smart grid technologies, which aim to integrate renewable energy sources into the grid and improve its efficiency and reliability. This is because converters need to be able to handle large power fluctuations and sudden changes of load [1]. In addition, they need to provide a stable voltage to the connected equipment. Additionally, the converters must also be able to regulate the power flow between the network and DGs, ensuring the network is not overloaded. The switching frequency of inverters must be carefully selected in order to match the operating voltage of the connected equipment, as well as the frequency of the network. Furthermore, the inverters must also be designed with the capability to handle sudden changes in load, such as when the DGs are switched on or switched off. If the inverters are not properly configured, the power quality problems will be severe, resulting in equipment damage and potential blackouts [2]. The algorithms are designed to optimize the placement of the DGs in a way that will ensure the quality of the power supplied to the grid. This optimization will ensure that the sudden changes in load are not too drastic and the inverters will be able to handle them without causing any power quality problems [3]. The algorithms are designed to look at the power demand and current supply and then calculate the best way to add the DGs to the grid in order to stabilize the power supply and demand. The additional devices help to provide more accurate information about the power supply and demand, which helps the algorithms to make more accurate calculations [4]. Two types of grid quality problems with electricity occur. Power outages, voltage fluctuations, voltage swells, voltage sags, imbalances, and harmonics are the primary causes of electrical problems. In addition, electric arc furnaces and UPS systems are examples of non-linear loads that might cause issues with the network current they draw. Issues with power quality such as imbalanced currents, harmonics, high reactive power, and inappropriate power factor can arise. A distinct division of labor among the various players is also essential for the liberalization of transportation networks. Furthermore, FACTS devices can aid in the prevention of overloading and conflicts caused by competing demands [5-8], in addition to enabling more accurate control over power flows. As a means of future-proofing and optimizing transportation networks, FACTS devices will be more crucial. When it comes to transmission systems, FACTS devices are king, but D-FACTS devices can be utilized in distribution systems as well. Determining the ideal mix of the three characteristics—type, placement, and size—of FACTS devices is critical to increasing their performance

[1]*Research Scholar, EE Department, University College of Engineering, Osmania University, Hyderabad*
swarna.kandukuri2007@gmail.com
[2]*Professor, EE Department, Vasavi College of Engineering, Hyderabad*
pmsarma2010@gmail.com
[3]*Professor, EE Department, University College of Engineering, Osmania University, Hyderabad*
majulagooga@gmail.com

[9]. 26 OnBasically, there are a lot of different reasons why power quality problems can occur. Conversely, the kind of disruption might have varying effects on the network and its users across the disruption mechanism. Accordingly, related standard-setting efforts and power quality studies attempt to classify the aforementioned disturbances according to their characteristics [10]. The power network now includes a wide range of non-linear loads that are not sinusoidal, thanks to the proliferation of power electronic device technologies. The waveform deviates from the ideal condition at rated frequency due to the presence of these loads, resulting in power quality distortion. However, intelligent electronic and microprocessor systems now regulate a great deal of loads. Network interruptions can rapidly degrade the operation of these systems [11], [12]. If you want to know how much voltage, current, and frequency distortion there is, look no further than power quality. Power quality is now receiving a lot more attention because electrical equipment is becoming more sensitive and because improving the power system's overall efficiency is becoming more important. International organizations such as the IEC, IEEE, and ANSI have developed standards for power quality indicators that can be used to track the reliability of electrical power [13]. The imbalanced distribution of single-phase and nonlinear loads is the primary cause of voltage unbalance. Reasons for this include uneven short circuits or connecting single-phase loads in different phases of the network, among others. While connected to the grid, using current from just one phase causes an imbalance in the network current [14]. Because of the voltage imbalance induced by the unbalanced current flowing through the network impedance, the performance of loads connected to the network, especially induction motors and equipment with electronic power converters, would be low. This is a more complex problem now that renewable energy is becoming more widely used [15]. Active filters, whether shunt or series, and mixed filters that use both types of circuits are common tools for repairing voltage imbalance. One of the most effective ways to improve power quality is via a series active filter. This type of filter may separate the load from the voltage source, and the reference voltage determination method is crucial [16]. You may figure out the filter's general design and the amount of compensation you want by choosing the reference voltage determination technique. Shunt filters, such as reactive power static compensators and synchronous static compensators, are commonly used to correct imbalances by injecting a negative component [17].There are a number of solutions proposed to address the imbalance, but one of the problems is the high expense of buying and setting up the necessary equipment. Furthermore, the network and its control become more complex due to the complications of controlling each of them [18]. One of the most difficult tasks recently has been the installation of energy-efficient hybrid power systems in outlying locations. Researchers must prioritize the best scale and control method for this reliable and cost-effective alternative energy source because these installations have caused increasingly prominent PQ challenges. [19]. The benefits of hybrid systems in the modern power grid setting have piqued interest in studying them. It is difficult to compare and evaluate the different control approaches and systems in an accurate manner. The primary challenge of hybrid systems is grid integration, which is exacerbated by PQ difficulties caused by the variable nature of renewable energy resources [20]. The assessment of new technology STATCOM issues and PQ disturbances under dynamic load situations is demonstrated in simulation studies addressed in [21-22] for a 100 kW SPV grid-connected system. In particular, the utility-grid's active and reactive power demands are decreased by variable reactive power supply. The implementation of a sliding mode controller allows for the extraction of maximum power from the SPV array within 3 ms while ignoring PQ disturbances and preventing exceeded.

2. Facts devices and Algorithms for present work

Nowadays, Power electronics-based FACTS devices allow for more precise continuous control of power flows, which has several advantages, such as keeping load bus voltages within acceptable ranges, managing active and reactive electrical power flows in thermally constrained lines, enhancing safety measures, and running electrical systems near their capacity limits, among other benefits. Figure 1 shows the four primary categories of FACTS optimization problem-solving strategies found in the literature: several approaches to optimization, including classical, meta-heuristic, sensitivity index, and hybrid approaches.

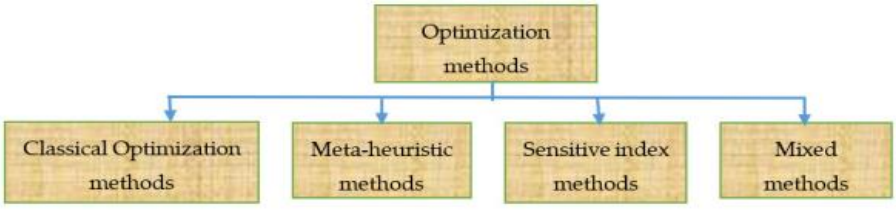

Fig 1: Power flow optimization methods

The current standard for finding the optimal placement, configuration, and dimensions of FACTS units is metaheuristic optimization. These methods are more user-friendly than the old ones when it comes to finding the best answer to difficulties. There are four ways to classify this group: (i) evolutionary algorithms such as genetic algorithms (GA) evolution strategy (ES) [23], evolutionary programming (EP) [24], genetic programming (GP) [25]; (ii) physics-based algorithms such as the ant lion optimization (ALO) technique [26], biogeography-based optimizer (BBO) [31], curved space optimization (CuSO) [29], flower pollination algorithm (FPA) [27], galaxy-based search algorithm (GBSA) [28], gravitational search algorithm (GSA) (iii) swarm-based algorithms such as particle swarm optimization (PSO) [29], whale optimization algorithm (WOA) [30], artificial bee colony (ABC) [31], chemical reaction optimization (CRO) algorithm [32], crow search algorithm (CSA) [33], cat swarm optimization (CaSO) algorithm [34], cuckoo search (CS) [35], etc.; and (iv) other population-based algorithms such as the black hole (BH) algorithm [36], parallel seeker optimization algorithm (PSOA) [37], imperialistic competitive algorithm (ICA) [38], sine cosine algorithm (SCA) [39,40], teaching–learning-based optimization (TLBO) algorithm. When they're out in nature, animals hunt for food at random. Because an animal's next move is dependent on its present position/state and the transition probability to its next place, its foraging path is typically just a random walk. Its decision-making process is underpinned by a mathematically-modelable probability.

2.1 Power law equations for present work

$$P_{k+1} = P_k - P_{loss,k-P_{Lk+1}}$$

$= P_k - \frac{R_k}{|V_k|^2}\{P_k^2 + (Q_k + Y_k|Y_k|^2)^2\} -$
P_{LK+1}…….. (1)

$$Q_{k+1} = Q_k - Q_{loss,k-P_{Lk+1}}$$

$=Q_k - \frac{X_k}{|V_k|^2}\{P_k^2 + (Q_k + Y_{k1}|Y_k|^2)^2\} - Y_{K1}|Y_k|^2 -$
$-Y_{k2}|V_{k+1}|^2 - -Q_{LK+1}$……..(2)

$$|V_{k+1}|^2 = |V_k|^2 + \frac{R_k^2 + X_k^2}{|V_k|^2}(P_k^2 + Q_k^2) - 2(R_k P_k + X_k Q_k$$

$=|V_k|^2 + \frac{R_k^2+X_k^2}{|V_k|^2}(P_k^2 + (Q_k^2 + Y_k|V_k|^2)^2 - 2(R_k P_k +$
$X_k(Q_k+Y_k|V_k|^2)^2$……..(3)

$P_{ij} = V_i^2 G_{ij} + V_i + V_j(B_{ij}Sin\delta_{ji} -$
$G_{ij}cos\delta_{ji})$…… (4)

$Q_{ij} = -V_i^2(B_{ij} + B_{sh}) + V_i V_j B_{ij} cos\delta_{ji} +$
$G_{ij}sin\delta_{ji})$…… (5)

$P_{ji} = V_j^2 G_{ij} - V_i V_j(G_{ij}cos\delta_{ji} +$
$B_{ij}sin\delta_{ji})$…… (6)

$Q_{ji} = -V_j^2(B_{ij} + B_{sh}) + V_i V_j(B_{ij}cos\delta_{ji} -$
$G_{ij}sin\delta_{ji}$…… (7)

Where

$\delta_{ji} = -\delta_j - \delta_i = -\delta_{ij}$…… (8)

PVR=$\frac{V_b}{V_o}$…….. (9)

3. Load conditions for base case

Base case inputs for IEEE 33 & 57 radial distribution bus systems are presented. IEEE 33 bus test system has 33 buses, 32 lines. The total real power demand is 3.715MW and reactive power demand is 2.3MVAR. Base case study is initiated with all buses voltage at 1pu and source (Bus1) is reference bus relatively to 57 bus system also with 57 buses and 56 lines.

3.1 Nature inspired algorithms for present work

Three algorithms chosen for optimal tracking and compensation for this comparative work in that first one is MBO(Monarch Butterfly Optimization) second is GWO(Grey Wolf Optimizer) and third one is CSO(Cuckoo Search optimization).

Monarch butterfly migration patterns in North America served as inspiration for and a source of inspiration for the MBO approach. The butterfly in this monarch swarm migrates from territories 1-2 in April and 2-1 in September. They create offspring that replace their parents in swarms at the time of emigration. Additionally, this MBO model includes two updated operators named the migration operator and the butterfly adjustment. This model continues to run until the required operational conditions are met. Various common functions have been projected using this paradigm. Further, for complicated standard functions like average fitness and standard deviation, the standard MBO version shows considerable technological limits. Zd is the step size of the butterfly walk y, which can be generated by dZ=levy (Z t) Levy flight, and BAR represents the butterfly adjustment rate. In addition, the performance metric denoted as α has been used as a balancing factor.

$\alpha = W_{max}/t^2$

Step 1: Collect a flexible and randomly created monarch swarm population of butterflies (NP), divide it into two parts (NP2 and NP1), and then configure the algorithm using parameters like BAR and Wmax, the maximum number of iterations.

Step 2: Find the fitness value of every monarch butterfly population.

Step 3: Organize the butterflies into two populations, NP1 and NP2, for territories 1 and 2, respectively, based on their fitness scores.

Step 4: The process of fertilization in Population NP1 in Territory 1 occurs as a result of operators' insatiable need for population growth. Similarly, NP2, the population of territory 2, modifies the operator of the butterfly algorithm with operators of the adaptive crossover scheme and the greedy algorithm to produce new generation.

Step 5: Design a correction method to fix any butterflies caused by impossible individuals.

Step 6: When a superior person is found, upgrade the effective individual butterfly.

Step 7: Repeat steps 2 through 6 as many times as necessary to reach the maximum

number of stopping criteria or iterations.

Grey wolf optimizer (GWO) It is a population-based meta-heuristics algorithm that was proposed in 2014 by Seyedali Mirjalili et al. and mimics the natural hunting mechanism and leadership hierarchy of grey wolves. The grey wolf is at the very pinnacle of the food web as an apex predator. Grey wolves typically inhabit in social groups called packs, with an average of 5 to12 members per pack.

Main phases of Grey wolf hunting:

1. Locating, chasing, and approaching prey.

2. Encircling the prey and harassing it until it stops moving.

3. Predation on the prey

Cuckoo search (CS) It was impacted by the fact that certain cuckoo species are obligate brood parasites, meaning they deposit their eggs in the nests of other species of birds. It is possible for some host birds to fight cuckoos head-on. Take a host bird as an example. If it finds out the eggs aren't its own, it has two options: either discard the eggs or leave the nest and start over somewhere else. Also, some species have incredible timing when it comes to laying eggs. The host bird's nest is a common target for parasitic cuckoos. Eggs laid by cuckoos typically hatch just a little bit before those laid by their hosts. The first thing a cuckoo chick will do after hatching is to raise its share of food from its host bird by evicting the host eggs from the nest by blindly propelling them out. Research also shows that cuckoo chicks can imitate their host chicks' calls to increase their chances of feeding.

Cuckoos only release eggs in nests that are picked at random. Optimal nests with high-quality eggs will be passed down through generations. When there is a fixed number of host nests, the host bird has a probability of Pa e (0, 1) to detect the cuckoo's egg. To avoid further calculations, the host bird uses a set of worst nests to run the discovery operation on. Finding new solutions to the general problem using Levy flights and random walks is an important challenge. When generating new solutions.

$$X_i^{(t+1)} = X_i^{(t)} + \alpha \oplus \text{Levy}(\lambda)$$

α, which is greater than zero, represents the step size that ought to be associated with the relevant problem scales. For the majority of instances, we can utilize α = 1. Using a Levy distribution to determine the random step length, the Levy flight efficiently produces a random walk.

$$\text{Levy} \sim U = t^{\lambda}, \quad (1 < \lambda \leq 3)$$

Which has an infinite variance with an infinite average. This process resembles a random walk, but with steps that follow a power-law distribution and a heavy tail. To make the local search go more quickly, Levy should produce some fresh options by walking around the best one that has been used so far. Yet, to avoid being stuck in a local optimum, it is recommended that a significant portion of the new solutions be generated by far field randomization. These solutions should be located sufficiently distant from the current best solution.

3.2 Problem formulation and design

Positive effects of DG include an improved voltage profile, and negative effects include an increase in system losses. This work aims to execute the suggested strategy in a way that maximizes the beneficial effects and minimizes the negative ones. There are two indices that show the voltage profile: the desired value deviation (VI1) and the initial network voltage variation (VI2) without DG. The objective is to minimize the target value deviation and increase the current variation. The objective function proposed in this study is defined as

$$\text{OF} = \text{Min}[(W_L * \text{power loss}) + (W_{V1} * VI_1) - (W_{V2} * VI_2)]$$

Power loss weighting factor (WL), visual information weighting factor (WV1), and visual information weighting factor (WV2) are all defined here. A thorough description of each part will be provided. When power goes out at every node in the network, it adds up. A definition of total power loss would so be

$$\text{Power loss} = \frac{1}{\text{MVA base}}\left(\sum_{i=1}^{N}\sum_{j=1}^{N}(V_i - V_j) \times I_{ij}\right)$$

The voltage deviations index can be defined as follows

$$VI_1 = \frac{1}{N}\sum_{i=1}^{N}\left(\frac{|V_i - V_{\text{target}}|}{V_{\text{target}}}\right)$$

$$VI_2 = \frac{1}{N}\frac{\sum_{i=1}^{N}|V_i^{DG} - V_i^{no}|}{\sum_{i=1}^{N}V_i^{no}} \times 100$$

$$OF = \text{Min}\left[\left(W_L * \frac{1}{\text{MVA base}}\left(\sum_{i=1}^{N}\sum_{j=1}^{N}(V_i - V_j) \times I_{ij}\right)\right) + (W_{V1} * VI_1) - (W_{V2} * VI_2)\right]$$

The current between buses i and j is denoted as Iij, while the voltages at buses i and j are Vi and Vj, respectively. The voltage at bus i with DG is VDG i, and the voltage at bus i without DG is Vno i. In this case, N represents the overall bus workforce.

Here are the operational limitations:

Voltage limitation: $V_{min} \leq V_i \leq V_{Max}$

The voltage at bus i is represented by Vi, whereas Vmin and Vmax are the lowest and highest voltages that can be selected with a tolerance of ±5% per cent. Power is balanced by the following factors: Ng is the total number of traditional generation units; NDG is the total number of distributed generation units; Pggw/DG is the operating active power of conventional generation units g with DG; Pgd is the operating active power of distributed generation units d; Pd is the total load demand; and PL is the total active power loss.

$$\sum_{g=1}^{N_g} Pg_{gw/DG} + \sum_{d=1}^{N_{DG}} Pg_d = P_d + P_L$$

Active and reactive power: Qgi and Sgi,max are reactive and apparent power of the i_{th} DG the equation is as follows.

$$P_{gi}^2 + Q_{gi}^2 \leq S_{gi,max}^2$$

3.3 Mat lab simulation

Two models has been designed one for 33 and another for 57 bus systems for Mat-lab/Simulink simulations for optimal tracking and compensation.

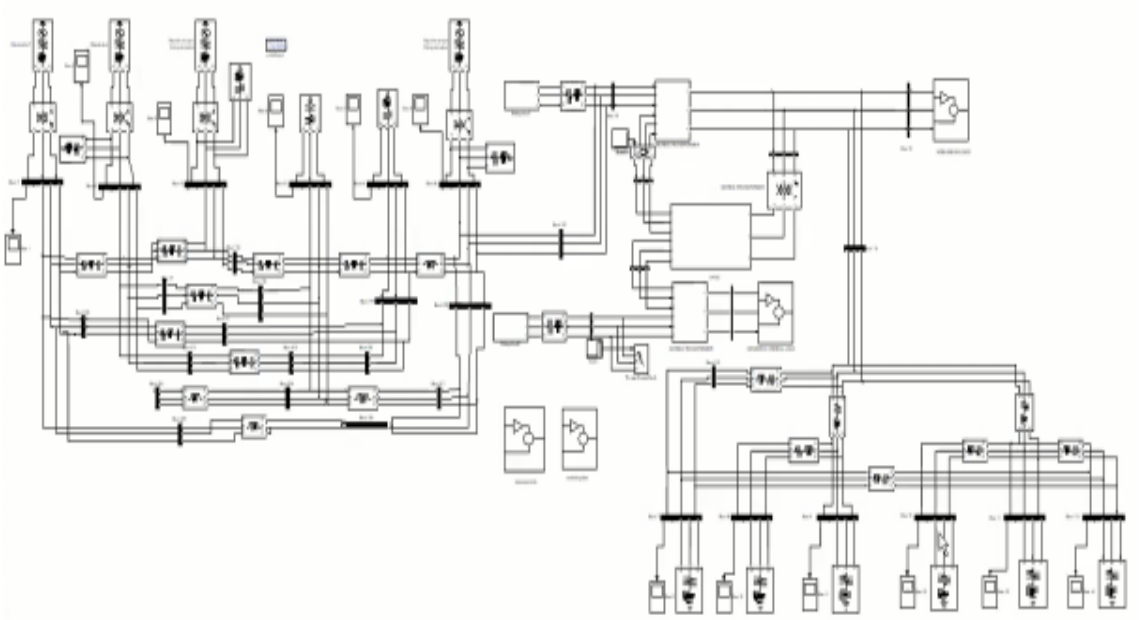

Fig:2 Design of 33 bus system

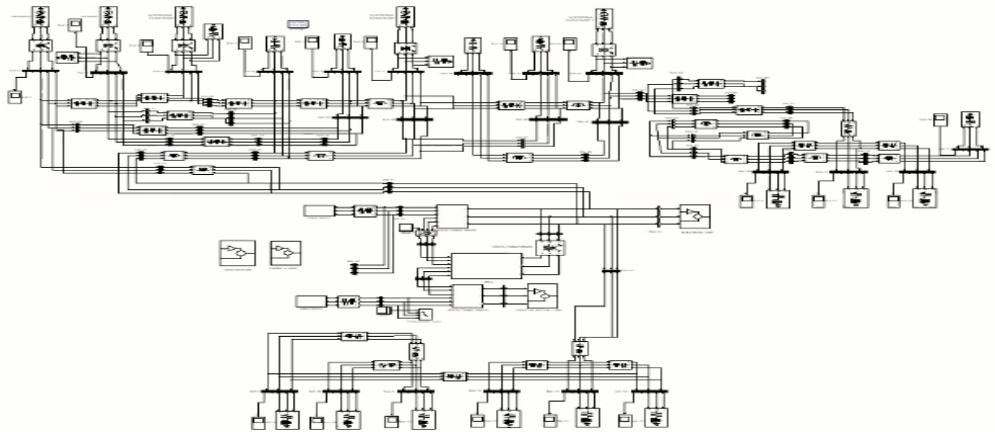

Fig:3 Design of 57 bus system

4.Results And Discussions

Optimization algorithm MBO is used for allocating DG based DSTATCOM indistribution network and to allocate DG based DSTATCOM & DVR the Grey Wolf Optimization is used and compared with Cuckoo search algorithm. Entire methodology utilizes MATLAB programming and simulation. With an objective of reduction of power losses performance parameters like RMS voltages during sag and swell and THD are studied. Base case results of IEEE 33 & 57 radial distribution bus systems are presented.

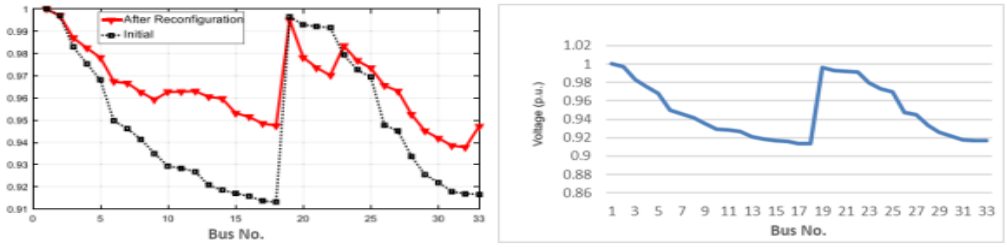

Fig 4 Optimal tracking for DG allocation using Cuckoo search and MBO algorithms in 33-Bus system

The total real power demand is 3.715MW and reactive power demand is 2.3MVAR. Base case study is initiated with all buses voltage at 1pu and source (Bus1) is reference bus. The least voltage occurs at 18th Bus and the voltage profile is shown in fig.5.

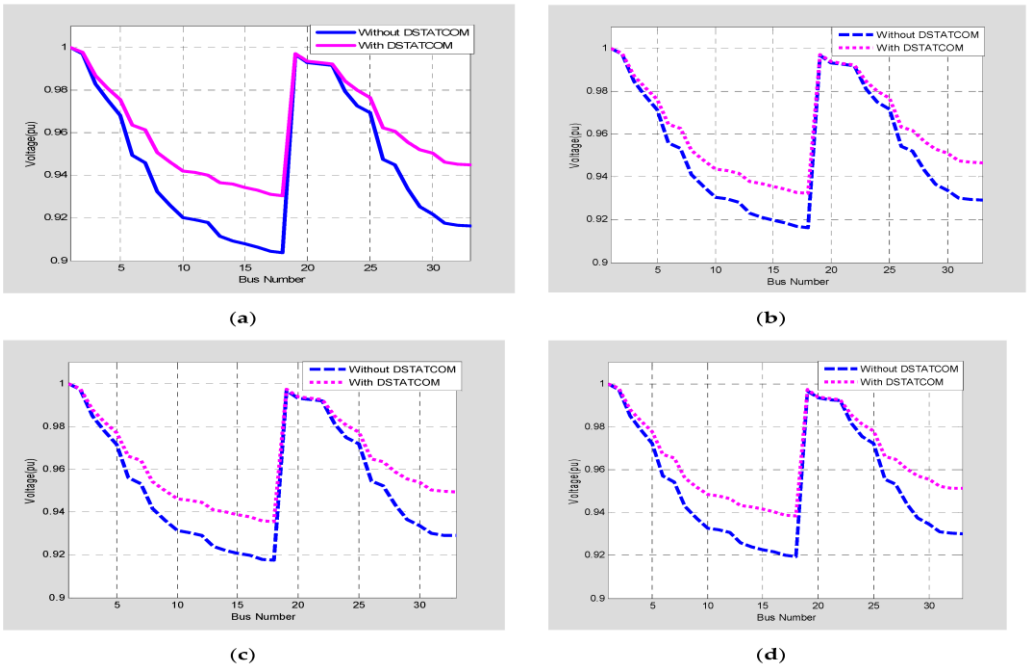

Fig 5: Voltage profile of standard 33-bus test system under different load models: (a) Constant Load, (b) Industrial Load, (c) Residential Load, and (d) Commercial Load.

Different load conditions were checked with Cuckoo search algorithm to find out optimal placement with the addition of fact device D-STAT COM observed and the problem find at 18th bus even though the fact device added.

Table:1 Line Losses in IEEE 33 bus test system

Line No.	Real Power Loss (kW)	Reactive Power Loss (kVAr)
1	12.3	6.27
2	52.076	26.524
3	20.053	10.213
4	18.85	9.6
5	38.565	33.291
6	1.946	6.433

7	11.873	8.569
8	4.266	3.065
9	3.634	2.576
10	0.565	0.187
11	0.899	0.297
12	2.721	2.141
13	0.744	0.98
14	0.364	0.324
15	0.287	0.21
16	0.257	0.343
17	0.054	0.043
18	0.161	0.154
19	0.832	0.75
20	0.101	0.118
21	0.044	0.058
22	3.182	2.174
23	5.144	4.062
24	1.288	1.007
25	2.602	1.325
26	3.33	1.696
27	11.305	9.968
28	7.810	6.827
29	3.897	1.985
30	1.594	1.576
31	0.213	0.249
32	0.013	0.105

Total Real power Loss is 210.97kW and total Reactive power Loss is 143.12kVAr. Line No. 2 sees the highest losses Similarly load flow analysis is conducted on 57 bus radial distribution networks shown in fig5. system has 57 buses, 56 lines. The total real power demand is 3802 kW and reactive power demand is 2694.6kVAr. Base case study is initiated with all buses voltage at 1pu and source (Bus1) is reference bus. The least voltage occurs at 39th Bus and value 0.9465679p.u and the voltage profile is shown in fig. Real and reactive power loss also computed maximum loss is seen in lines 2 and 3. Total real and reactive power loss are 158.45kW & 99.9kVAr.

Fig 6: Optimal tracking for DG allocation for 57- bus system

Table:2 Load flow Results of IEEE 57 Bus Test System

Bus No.	Voltage Magnitude in p.u	Voltage Angle in Degrees
1	1	0
2	0.9988	-0.16634
3	0.9862	-0.40998
4	0.9772	-1.5364

5	0.9772	-1.57876
6	0.9758	-0.39094
7	0.9756	-4.46798
8	0.9731	-0.70153
9	0.9705	-1.00592
10	0.9704	-0.27266
11	0.9672	-1.27298
12	0.9703	-2.01714
13	0.9667	-0.54924
14	0.9663	-0.47559
15	0.9665	-0.30185
16	0.9703	-0.36111
17	0.9702	-0.66277
18	0.9734	-1.45933
19	0.9713	-1.72039
20	0.9692	-1.23039
21	0.9668	-0.54311
22	0.9645	-0.14394
23	0.9625	-0.63163
24	0.9612	-1.29145
25	0.9608	-1.49058
26	0.9607	-1.65342
27	0.9606	-1.71263
28	0.9606	-1.76181
29	0.9605	-1.7739
30	0.9601	-2.17979
31	0.9545	-1.0337
32	0.9538	-1.68263
33	0.9538	-2.2509
34	0.9534	-1.88271
35	0.9531	-2.07851
36	0.9523	-2.9594
37	0.9496	-2.37172
38	0.9468	-0.14543
39	0.9466	-0.32615
40	0.9523	-3.5364
41	0.9661	-3.49617
42	0.9659	-4.14021
49	0.9638	-2.85683
50	0.9637	-2.6317
51	0.9637	-2.53461
52	0.9601	-1.18117
53	0.9601	-1.27545
54	0.9601	-0.85371
55	0.9601	-0.89107
56	0.9521	-1.95243
57	0.9487	-0.26642

4.1 Implementation of MBO algorithm for optimal DG with DSTATCOM allocation

From the Load flow it is observed that minimum voltage bus (18^{th}) sees a voltage was 0.913p.u. Buses 6 to 18 and 26 to 33 have undergone low voltages. Whereas for 57 bus test system bus 39 is the least voltage bus 0.9465p.u and five buses namely 37,38,39,44 and 57 buses have undergone low voltages below 0.95p.u. Optimization problem for installation of DG with DSTATCOM for loss

minimization is resolved with MBO (Monarch Butterfly Optimization) algorithm. According to MBO, bus number 18th is the best location for 33 bus test system and for 57 bus test system 30th bus is the optimal location for installing the DSTATCOM. During certain conditions the optimal locations will changed.

Table 3: Voltage Magnitudes of IEEE 33 Bus test system

Bus No	Base Case	DG	DSTATCOM	DG WITH DSTATCOM
1	1	1	1	1
2	0.997	0.999	0.9977	0.9996
3	0.983	0.9954	0.9873	0.9991
4	0.9755	0.9935	0.9825	0.9987
5	0.9681	0.992	0.9771	0.9988
6	0.9497	0.9863	0.9658	0.9988
7	0.9462	0.9837	0.9636	0.9975
8	0.9414	0.9819	0.9593	0.9959
9	0.9351	0.9799	0.9547	0.9951
10	0.9293	0.9784	0.9506	0.9948
11	0.9284	0.9784	0.9499	0.9948
12	0.9269	0.9784	0.9487	0.995
13	0.9208	0.9783	0.9451	0.9967
14	0.9186	0.9783	0.9443	0.9979
15	0.9172	0.9792	0.9441	0.9997
16	0.9158	0.9779	0.9427	0.9984
17	0.9138	0.976	0.9408	0.9966
18	0.9132	0.9755	0.9402	0.996
19	0.9965	0.9985	0.9972	0.999
20	0.9929	0.9949	0.9936	0.9955
21	0.9922	0.9942	0.9929	0.9948
22	0.9916	0.9936	0.9923	0.9941
23	0.9794	0.9919	0.9837	0.9955
24	0.9727	0.9853	0.9771	0.989
25	0.9694	0.982	0.9737	0.9857
26	0.9478	0.9845	0.9639	0.997
27	0.9452	0.982	0.9614	0.9946
28	0.9338	0.971	0.9501	0.9837
29	0.9256	0.9631	0.942	0.9759
30	0.922	0.9597	0.9386	0.9726
31	0.9179	0.9557	0.9345	0.9686
32	0.9169	0.9548	0.9336	0.9678
33	0.9167	0.9545	0.9333	0.9675

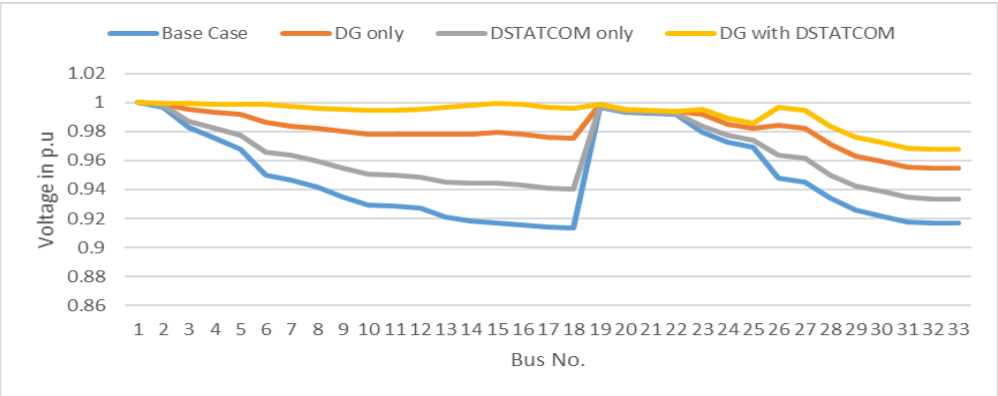

Fig 7: Voltage profile of 33 bus test system with DG based Compensation

Line losses are seen as 30.13 kW and 27.43kVAr. Losses in line 2 are reduced to 3kW and high losses are seen in 1st line. With DSTATCOM only few buses voltages (12 to 18 and 29 to 33) are below 0.95p.u and hence both are installed together and better performance is seen as expected. The performance indices considered are tabulated in table

Table4: Performance Indices with installation of Devices at optimal location

	Base Case	DG	DSTATCOM	DG WITH DSTATCOM
Least voltage &bus	0.9132p.u at 18th Bus	0.9545p.u at 33rd bus	0.933p.u at33rd Bus	0.9675p.u at33rd Bus
Total Real Power losses	210.97kW	113.15kW	151.47kW	30.13kW
Total Reactive Power losses	143.12kVAr	102.33kVAr	89.8kVAr	27.43kVAr

Table 5: Voltage Magnitude of IEEE 57 Bus test system

Bus No	Base Case	DG	DSTATCOM	DG WITH DSTATCOM
1	1	1	1	1
2	0.9988	0.999	0.9999	0.9996
3	0.9862	0.9954	0.99873	0.9991
4	0.9772	0.9935	0.99825	0.9987
5	0.9772	0.992	0.99771	0.9988
6	0.9758	0.9863	0.99658	0.9988
7	0.9756	0.9837	0.99636	0.9975
8	0.9731	0.9819	0.98593	0.9959
9	0.9705	0.9799	0.98547	0.9951
10	0.9704	0.9784	0.98506	0.9948
11	0.9672	0.9784	0.98499	0.9948
12	0.9703	0.9784	0.98487	0.995
13	0.9667	0.9783	0.98451	0.9967
14	0.9663	0.9783	0.98443	0.9979
15	0.9665	0.9792	0.98441	0.9997
16	0.9703	0.9779	0.98427	0.9984
17	0.9702	0.976	0.98408	0.9966
18	0.9734	0.9755	0.98402	0.996
19	0.9713	0.9985	0.9972	0.999
20	0.9692	0.9949	0.9936	0.9955
21	0.9668	0.9942	0.9929	0.9948
22	0.9645	0.9936	0.9923	0.9941
23	0.9625	0.9919	0.9837	0.9955
24	0.9612	0.9853	0.9771	0.989
25	0.9608	0.982	0.9737	0.9857
26	0.9607	0.9845	0.9839	0.997
27	0.9606	0.982	0.98614	0.9946
28	0.9606	0.971	0.9801	0.9837
29	0.9605	0.9631	0.9652	0.9759
30	0.9601	0.9597	0.96386	0.9726
31	0.9545	0.9557	0.96345	0.9686
32	0.9538	0.9548	0.9636	0.9678
33	0.9538	0.9545	0.9633	0.9675
34	0.9534	0.9783	0.98443	0.9979

35	0.9531	0.9792	0.98441	0.9997
36	0.9523	0.9779	0.98427	0.9984
37	0.9496	0.976	0.98408	0.9966
38	0.9468	0.9755	0.98402	0.996
39	0.9466	0.9985	0.9972	0.999
40	0.9523	0.9949	0.9936	0.9955
41	0.9661	0.9942	0.9929	0.9948
42	0.9659	0.9936	0.9923	0.9941
43	0.9659	0.9919	0.9937	0.9955
44	0.9465	0.9853	0.9871	0.989
45	0.9662	0.982	0.9837	0.9857
46	0.9650	0.9845	0.98639	0.997
47	0.9638	0.982	0.98714	0.9946
48	0.9635	0.971	0.97501	0.9837
49	0.9638	0.9631	0.969	0.9759
50	0.9637	0.9597	0.9686	0.9726
51	0.9637	0.9557	0.96545	0.9686
52	0.9601	0.9548	0.96336	0.9678
53	0.9601	0.9545	0.96333	0.9675
54	0.9601	0.9783	0.98443	0.9979
55	0.9601	0.9792	0.98441	0.9997
56	0.9521	0.9779	0.98427	0.9984
57	0.9487	0.976	0.98408	0.9966

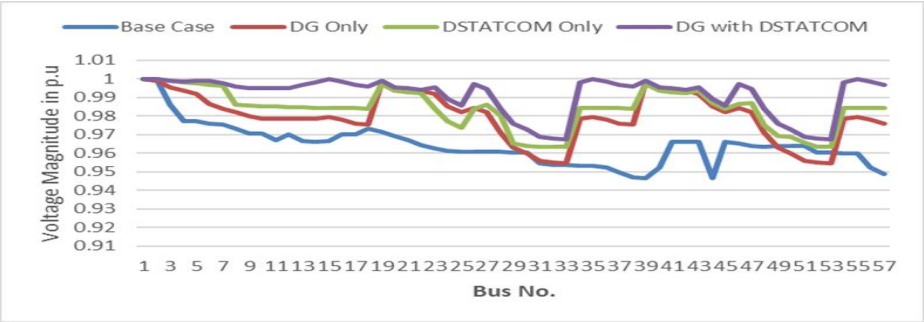

Fig 8: Voltage profile of 57 bus system with DG based Compensation

Line losses are seen as 17.01kW and 15.54kVAr. Losses in line 2 are reduced to 0.016kW and high losses are seen in 10th line. With DG & DSTATCOM all bus voltages are above 0.95p.u. This might be because of the optimal capacities of DG & DSTATCOM obtained are higher side. However to check the performance with both the devices after installation of DG & DSTACOM together many buses have reaches voltages above 0.98p.u.The performance indices considered are tabulated in table.

Table 6: Performance Indices with installation of Devices at optimal location

	Base Case	DG	DSTATCOM	DG WITH DSTATCOM
Least voltage& bus	0.9466p.u at 39th Bus	0.9545p.u at 33rd & 53rd buses	0.9633p.u at33rd & 53rd buses	0.9675p.u at 53rd bus
Total Real Power losses	158.64kW	125.6kW	102.5kW	17.01kW
Total Reactive Power losses	99.98kVAr	47.3kVAr	58.7kVAr	15.54kVAr

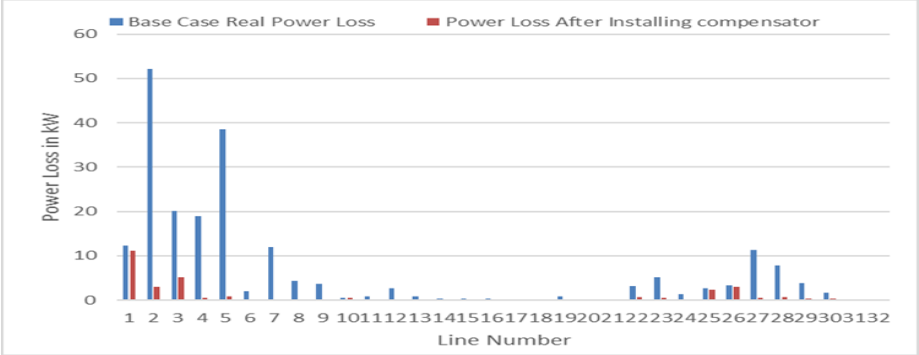

Fig 9: Power loss before and after Compensation for 33 bus test system

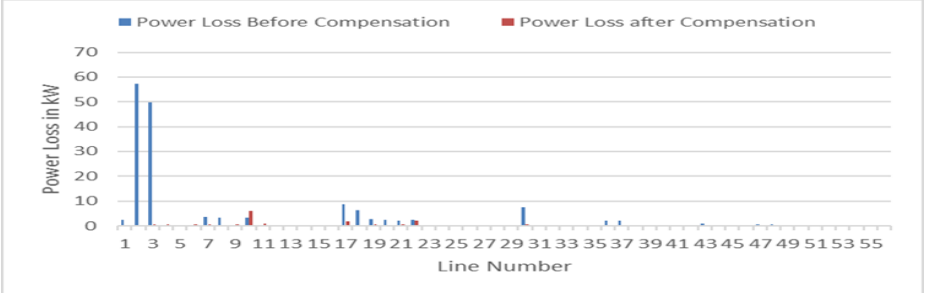

Fig 10: Power loss before and after Compensation for 57 bus test system

Dynamic behavior of the system in the presence of DSTATCOM along with DG is studied during the fault condition. Voltage sag or swell occurred for a duration of 0.2sec (i.e from 0.3sec to 0.5sec). Sag is created by a 3-phase fault, swell is created by switching on a series capacitor. The sag voltage, injected voltage and compensated voltage waveforms, for 33 and 57 bus systems are shown in Figs. 10 to 14. The RMS values of compensated voltage before and after compensation and injected current waveforms for 33 and 57 bus systems are shown in Figs 15 ,16,17.

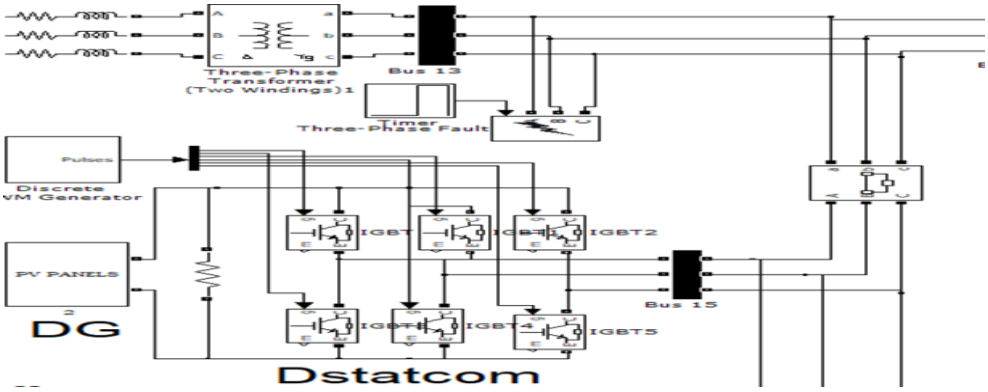

Fig 11: Installation of DSTATCOM along with DG at bus 18 for 33 bus system

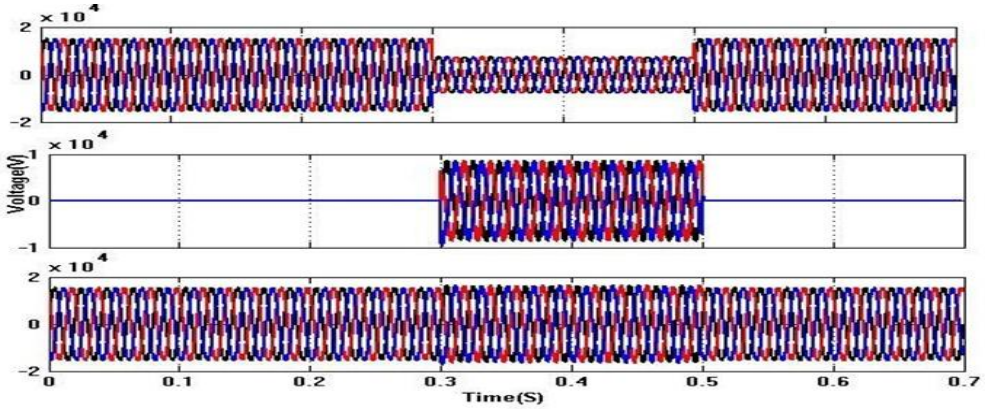

Fig12: Voltage profile (Vabc) at PCC: Sag voltage, DG based DSTATCOM injected voltage, Compensated Voltage at load 33 bus

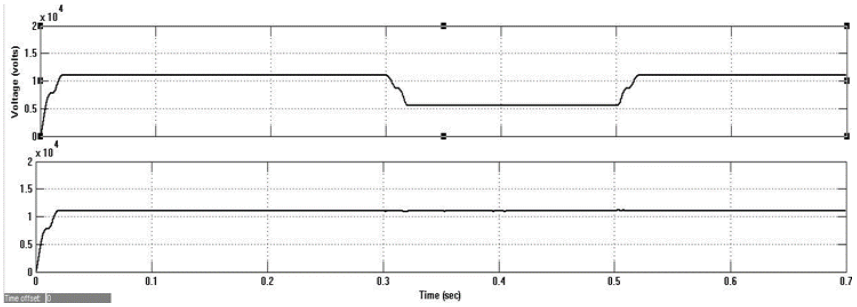

Fig 13: Voltage profile (Vrms) at pcc: Before & After compensation (Sag) for 33bus

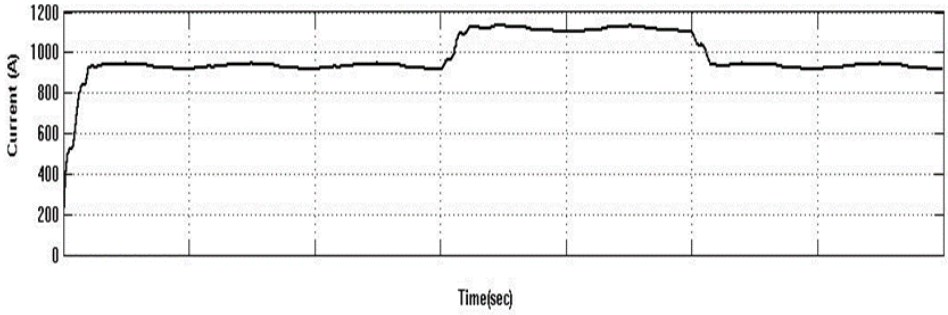

Fig 14: Current profile (Irms) at pcc: RMS Injected current for 33bus

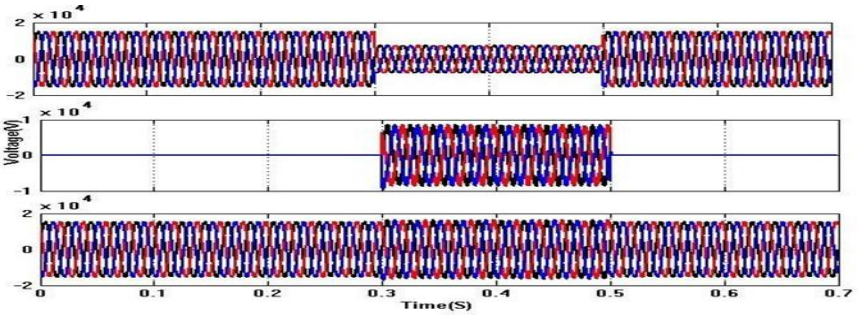

Fig 15: Voltage profile (Vabc) at pcc: Sag voltage, DG based DSTATCOM injected voltage, Compensated Voltage at load for 57 bus

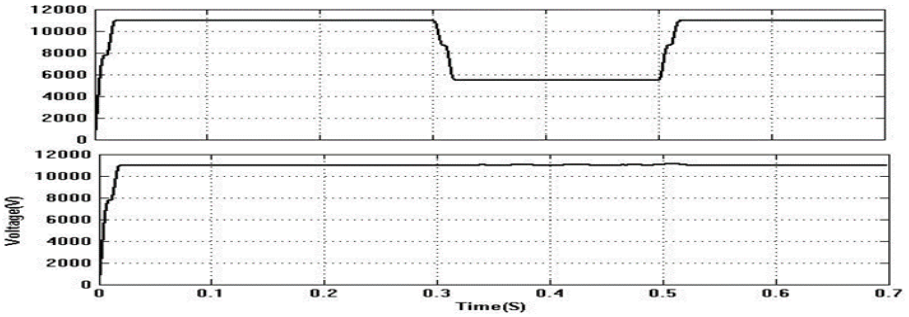

Fig 16: Voltage profile (Vrms) at pcc: Before & After compensation (Sag) for 57 bus

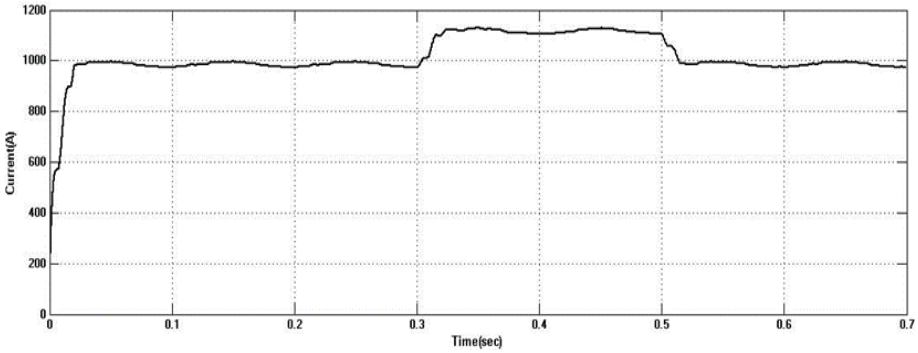

Fig 17: Current profile (Vrms) at pcc: RMS Injected current for 57 bus

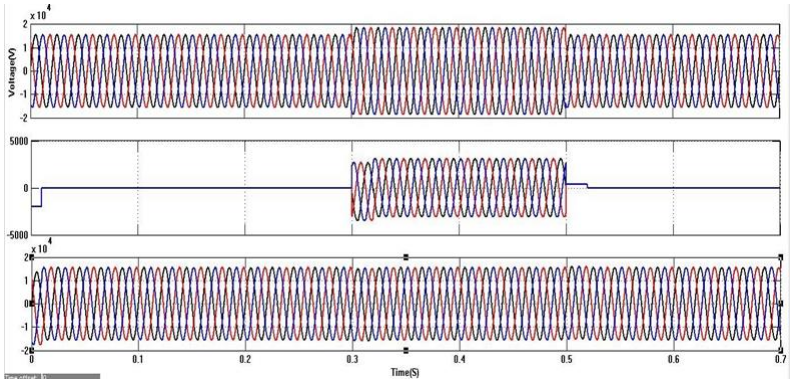

Fig 18: Voltage profile (Vabc) at pcc: Swell voltage, DG based DSTATCOM injected voltage, Compensated Voltage at load for 33bus.

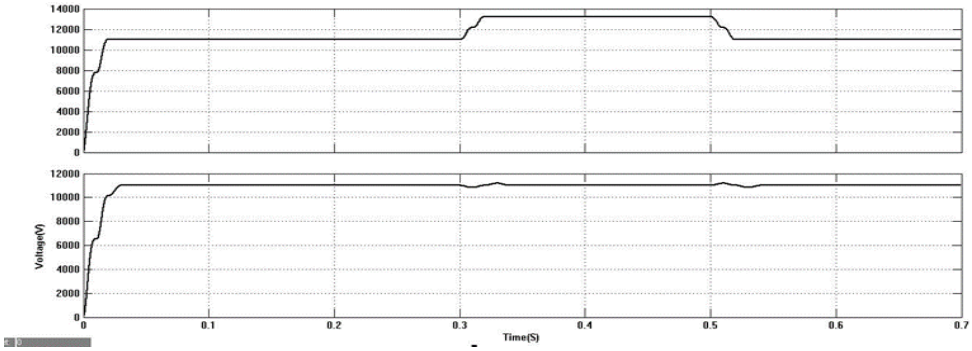

Fig 19: Voltage profile (Vrms) at pcc: Before & After compensation (Swell) for 33bus

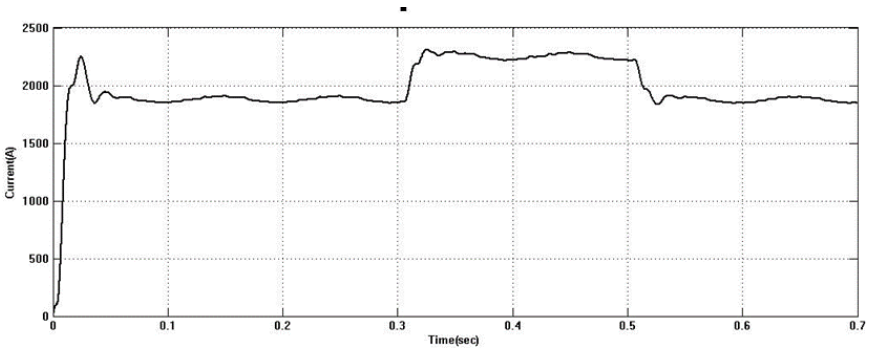

Fig 20: Current profile (Irms) at pcc: RMS Injected current for 33bus

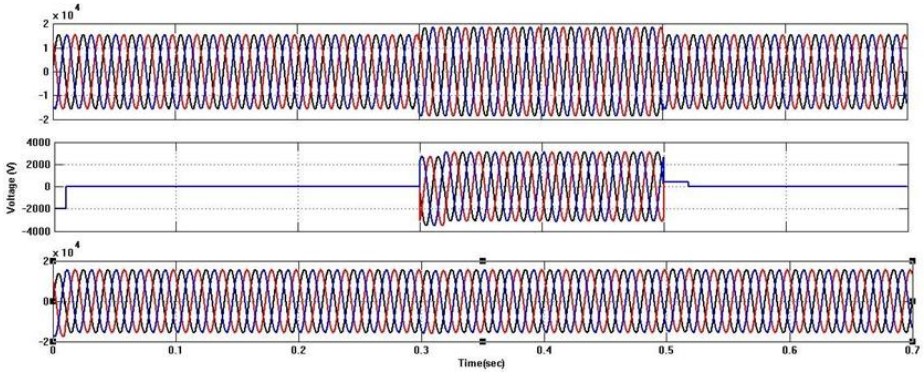

Fig 21: Voltage profile (Vabc) at pcc: Swell voltage, DG based DSTATCOM injected voltage, Compensated Voltage at load for 57 bus

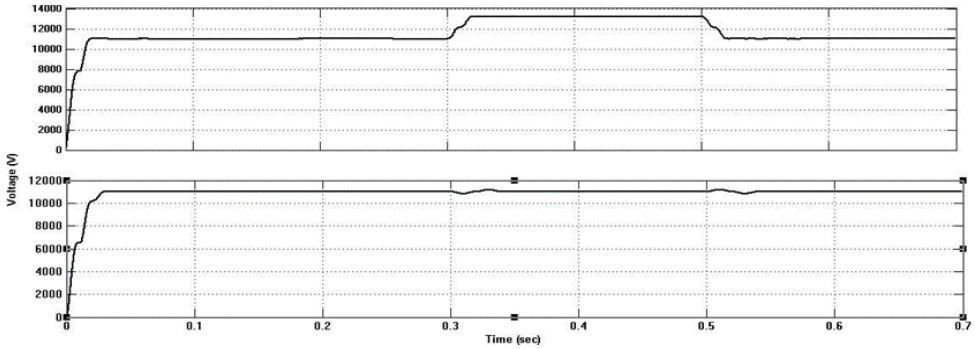

Fig 22: Voltage profile (Vrms) at pcc: Before & After compensation (Swell) for 57 bus

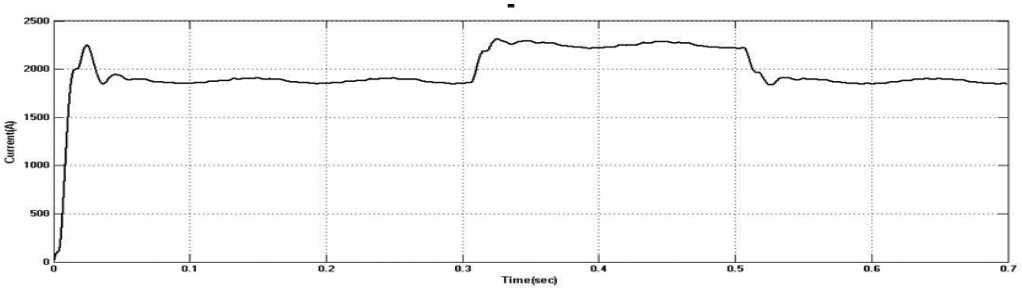

Fig 23: Current profile (Irms):RMS injected current at pcc for 57 bus

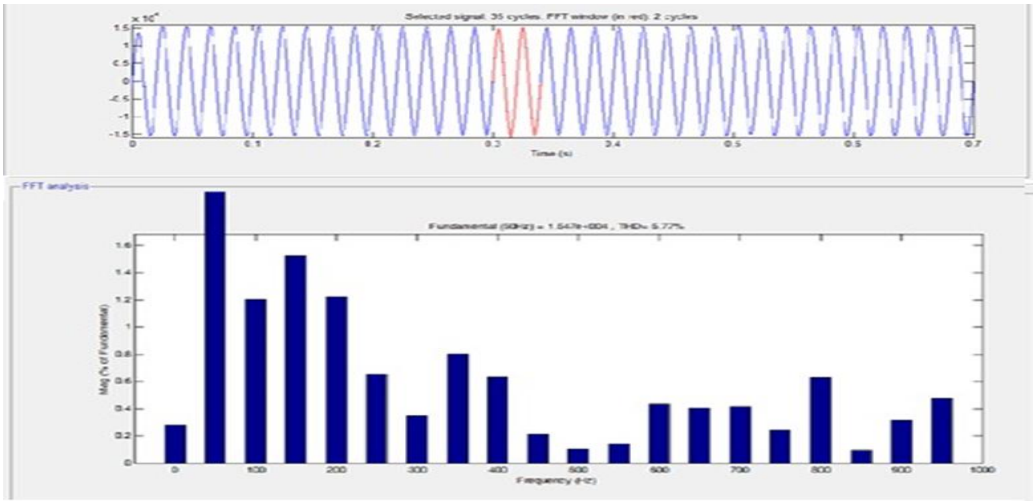

Fig 24: Voltage Total harmonic distortion of DG connected DSTATCOM i,e.

T.H.D=5.77%

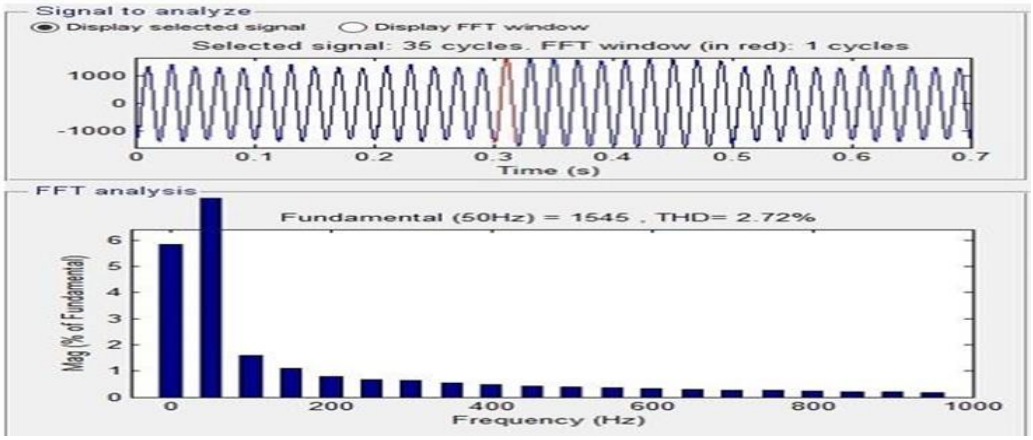

Fig:25 Current Total harmonic distortion of DG connected DSTATCOM i,e. T.H.D=2.72%

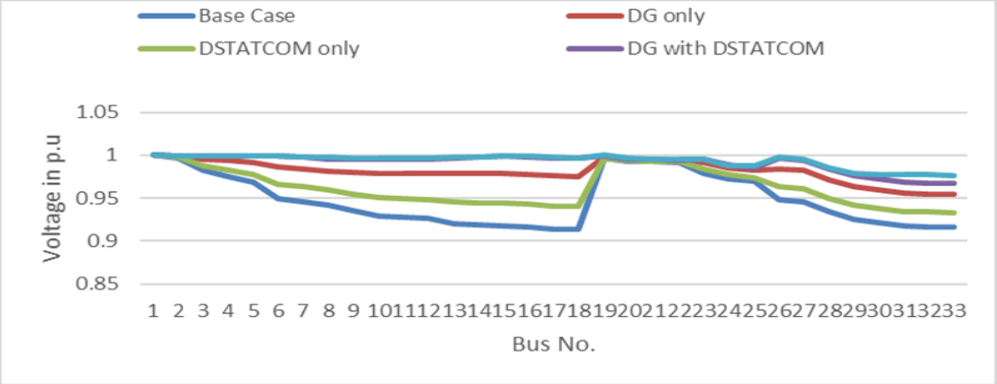

Fig 26 Voltage Profile of IEEE 33 Bus after installing DG based DSTATCOM & DVR

With DG based DSTATCOM & DVR only few buses voltages (31 to 33) are below 0.98p.u and hence both are installed together and better performance is seen as expected. The performance indices considered are tabulated in table

Table 7: Performance Indices with installation of Devices at optimal location

	Base Case	DG	DSTATCOM	DG with DSTATCOM	DG with DSTATCOM & DVR
Least voltage& bus	0.9132p.u at 18th Bus	0.9545p.u at 33rd bus	0.933p.u at 33rd bus	0.9675p.u at 33rd bus	0.9768p.u at 33rd bus
TotalReal Power losses	210.97kW	113.15kW	151.47kW	30.13kW	19.29kW
Total Reactive Power losses	143.12kVAr	102.33kVAr	89.8kVAr	27.43kVAr	9.88kVAr

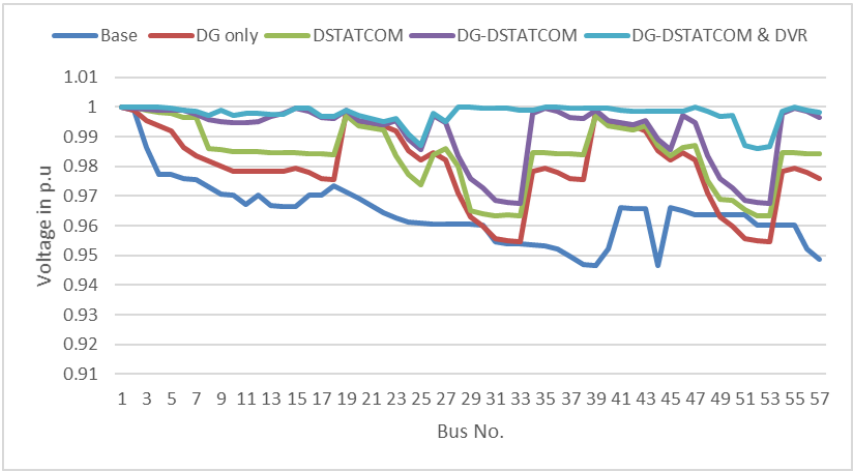

Fig 27 Voltage Profile of IEEE 57 Bus after installing DG based DSTATCOM & DVR

Table :8 Simulation outcomes with settling time, THD, % of sag & swell forIEEE 33 & 57 bus

S. No.	Compensator	Settling time (sec.)	V_{THD}	I_{THD}
1	DG (conventional)	0.1-0.6 (0.5sec)	12.7%	****
2	DG-DSTATCOM Sag Swell	 0.3-0.5 (0.2sec) 0.3-0.5 (0.2sec)	3.99%	2.72%

			5.77%	1.83%
3	GWO-DVR & MBO – DSTATCOM 33 bus Sag Swell	0.3- 0.5 (0.2sec) 0.3- 0.5 (0.2sec)	0.01% 0.41 %	1.44%
4	GWO-DVR & MBO – DSTATCOM 57 bus Sag Swell	0.3- 0.5 (0.2sec) 0.3- 0.5 (0.2sec)	0.01% 0.41%	0.29%

The THD of Voltage Sag & injected current at pcc for GWO fed DVR & MBO fed DSTATCOM are 0.01%, 2.72% for 33 bus and the FFT Analysis is shown in Fig. 28and the THD for Voltage Swell and the current at pcc are 0.41%, 0.29% for 57 bus is shown in Fig.29.

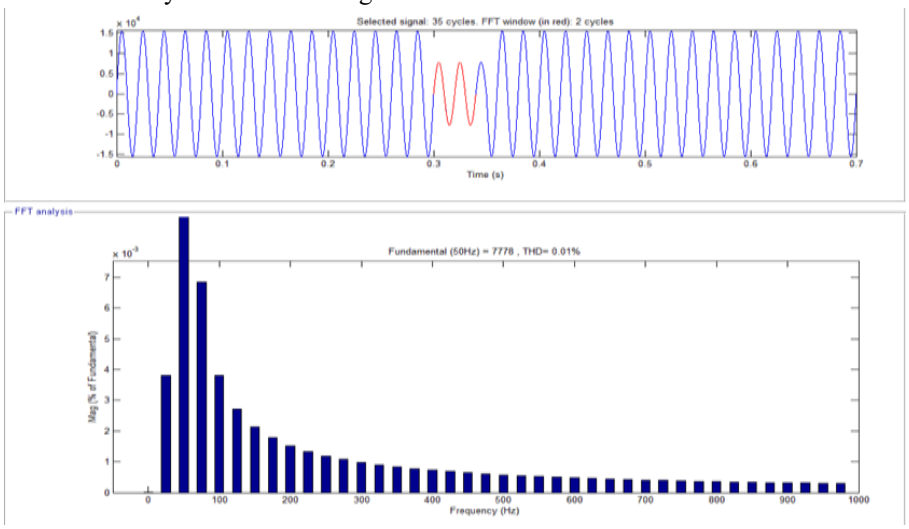

Fig 28: Total harmonic distortion of voltage for GWO with DVR & MBO with DSTATCOM i,e. T.H.D =0.01% for 33 bus

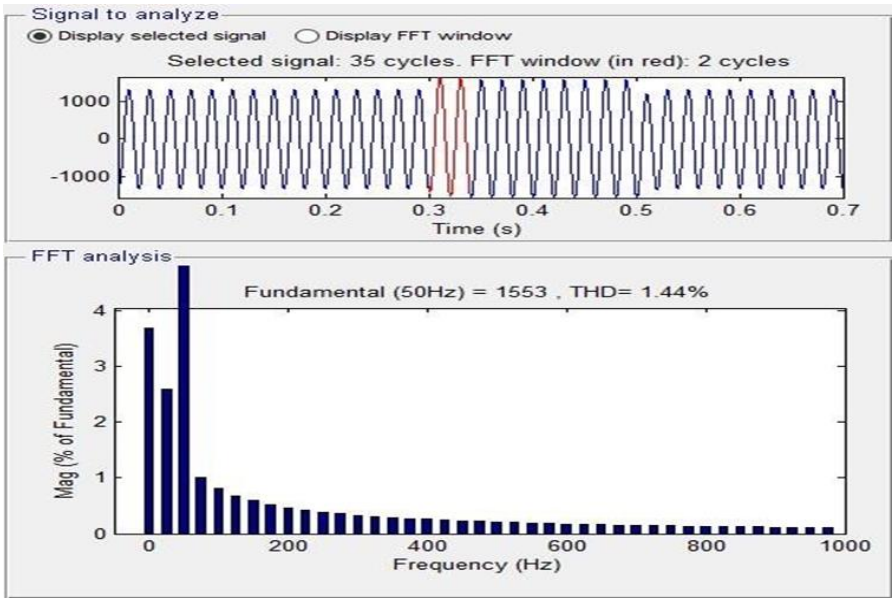

Fig 29: Current Total harmonic distortion of current for GWO - DVR & MBO-DSTATCOM i,e. T.H.D =1.44% for 33 bus

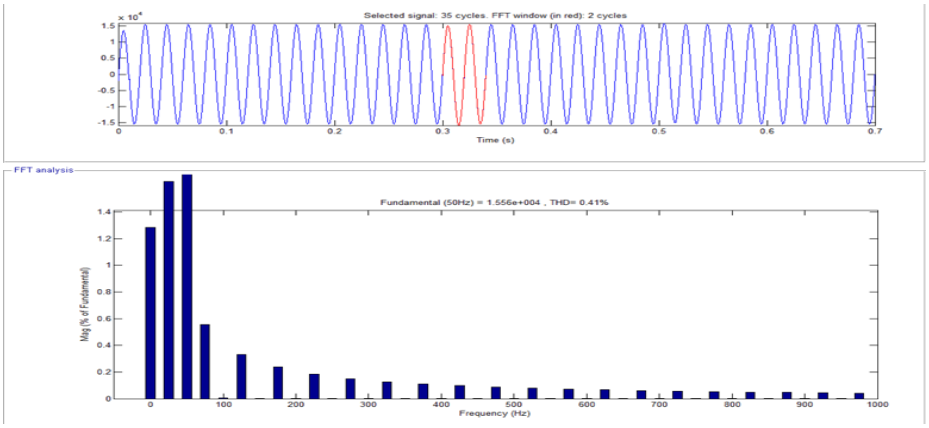

Fig 30: Total harmonic distortion of voltage for GWO -DVR & MBO-DSTATCOM i,e. T.H.D =0.41% for 57 bus

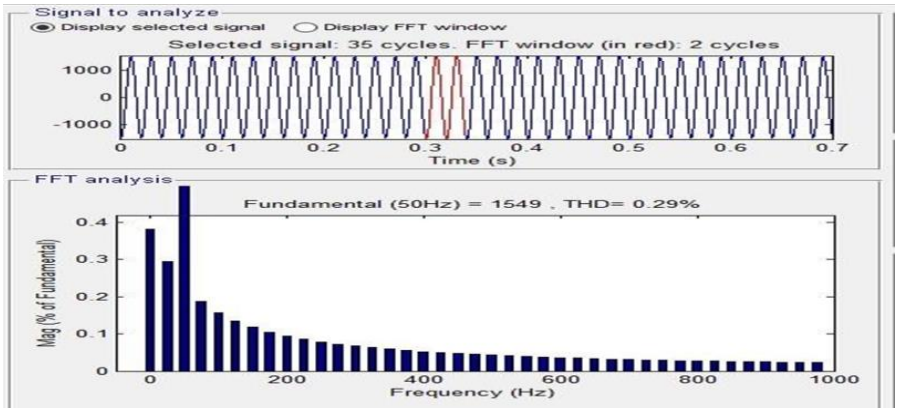

Fig 31: Current Total harmonic distortion of Current for GWO - DVR & MBO-DSTATCOM i,e. T.H.D =0.29% for 57 bus

5. Conclusions

Heuristic with nature inspired algorithms considered in the present work taken from the previous literature. The design of 33 and 57-bus systems with optimal tracking and compensation with fact devices. The following conclusions drawn from above simulation

- MBO and Cuckoo search algorithms are used for optimal tracking comparison in33 bus system to ensure the design responding in same for any algorithm. The two algorithms shows the voltage drop at 18th bus only with a deviation in PU value.
- The design further optimized with different load conditions the before compensation the power loss is 210KW, Vmin (pu)0.9037, VSI min(pu)0.6610 and the Kvar at different bus is 350,520,1010 taken for 100 runs, after compensation the average power loss decreased to 147.24KW with % reduction of 34.37 with minimum PU value of 0.9304.
- The addition of DG improves the power quality with MBO optimization. DG with DSTAT COM given better results than DSTAT COM.
- GWO algorithm with DVR added further to minimize the power loss, for smaller system the compensation is guaranteed, when it comes to 57 bus system there is still some disturbances at 25th and 50 buses.
- The work optimized with different algorithms in the present work to minimize power harmonic distortions. The implementation cost for the devices as well as approach leads high in economic prospectus the work can be optimized with hybrid algorithms(by adding AI based two optimal algorithms) with multi-converter based UPQC is the better scope for further researches is recommended.

References

[1] E. Fuchs and M. Masoum, "Introduction to power quality," in Power Quality in Power Systems and Electrical Machines, 2nd ed. Cambridge, MA, USA: Academic Press, 2015, pp. 1–104.

[2] R. Igual and C. Medrano, "Research challenges in real-time classification of power quality disturbances applicable to microgrids: A systematic review," Renew. Sustain. Energy Rev., vol. 132, Oct. 2020, Art. no. 110050,doi: 10.1016/j.rser.2020.110050.

[3] D. Li, T. Wang, W. Pan, X. Ding, and J. Gong, "A comprehensive review of improving power quality using active power filters," Electric Power Syst. Res., vol. 199, Oct. 2021, Art. no. 107389.

[4] M. Fatiha, M. Mohamed, and A.-A. Nadia, "New hysteresis control band of an unified power quality

conditioner," Electr. Power Syst. Res., vol. 81, no. 9, pp. 1743–1753, Sep. 2011.

[5] Y. Naderi, S. H. Hosseini, S. Ghassemzadeh, B. Mohammadi-Ivvatloo, M. Savaghebi, J. C. Vasquez, and J. M. Guerrero, "Power quality issues of smart microgrids: Applied techiniques and decision making analysis," in Decision Making Applications in Modern Power Systems. Cambridge, MA, USA: Academic press, 2020, pp. 89–119.

[6] Y. Naderi, S. H. Hosseini, S. G. Zadeh, B. Mohammadi-Ivatloo, J. C. Vasquez, and J. M. Guerrero, "An overview of power quality enhancement techniques applied to distributed generation in electrical distribution networks," Renew. Sustain. Energy Rev., vol. 93, pp. 201–214, Oct. 2018.

[7] F. H. Gandoman, A. Ahmadi, A. M. Sharaf, P. Siano, J. Pou, B. Hredzak, and V. G. Agelidis, "Review of FACTS technologies and applications for power quality in smart grids with renewable energy systems," Renew. Sustain. Energy Rev., vol. 82, pp. 502–514, Feb. 2018.

[8] A. Soomro, A. Larik, M. Mahar, A. Sahito, A. Soomro, and G. Kaloi, "Dynamic voltage restorer—A comprehensive review," Energy Rep.,vol. 7, pp. 6786–6805, Nov. 2021.

[9] O. Rahat, M. Saniei, and S. G. Seifossadat, "Modeling and new tuning of the distribution transformer-integrated passive power filter and its effects on the transformer performance and network power quality," Electric Power Syst. Res., vol. 214, Jan. 2023, Art. no. 108844.

[10] R. B. Gonzatti, S. C. Ferreira, C. H. Da Silva, R. R. Pereira, L. E. B. Da Silva, and G. Lambert-Torres, "Smart impedance: A new way to look at hybrid filters," IEEE Trans. Smart Grid, vol. 7, no. 2, pp. 837–846, Mar. 2016.

[11] M. Moghbel, M. A. S. Masoum, A. Fereidouni, and S. Deilami, "Optimal sizing, siting and operation of custom power devices with STATCOM and APLC functions for real-time reactive power and network voltage uality control of smart grid," IEEE Trans. Smart Grid, vol. 9, no. 6, pp. 5564–5575, Nov. 2018.

[12] H. Fujita and H. Akagi, "The unified power quality conditioner: The integration of series- and shunt-active filters," IEEE Trans. Power Electron., vol. 13, no. 2, pp. 315–322, Mar. 1998.

[13] A. Singh and M. Badoni, "Power quality issues, modeling, and control techniques," in Advances in Smart Grid Power System. Cambridge, MA,USA: Academic Press, 2021, pp. 299–329.

[14] D. Graovac, V. Katic, and A. Rufer, "Power quality compensation using universal power quality conditioning system," IEEE Power Eng. Rev., vol. 20, no. 12, pp. 58–60, Dec. 2000.

[15] D. Graovac, V. Katic, and A. Rufer, "Power quality problems compensation with universal power quality conditioning system," IEEE Trans.Power Del., vol. 22, no. 2, pp. 968–976, Apr. 2007.

[16] C. Babu and S. S. Dash, "Design of unified power quality conditioner (UPQC) to improve the power quality problems by using P-Q theory," in Proc. Int. Conf. Comput. Commun. Informat., Coimbatore, India, Jan. 2012, pp. 1–7.

[17] F. G. Montoya, A. García-Cruz, M. G. Montoya, and F. Manzano-Agugliaro, "Power quality techniques research worldwide: A review," Renew. Sustain. Energy Rev., vol. 54, pp. 846–856, Feb. 2016.

[18] Q.-N. Trinh and H.-H. Lee, "Low cost and high performance UPQC with four-switch three-phase inverters," J. Electr. Eng. Technol., vol. 10, no. 3, pp. 1015–1024, May 2015.

[19] Ashish, D.; Mukesh, K.G.; Malay, K.B.; Suraj, K.S.; Bojan, Đ.; Dragana, D.; Nikola, K. Optimal Placement and Size of SVC with Cost-Effective Function Using Genetic Algorithm for Voltage Profile Improvement in Renewable Integrated Power Systems. Energies **2023**, 16, 2637.

[20] Brindha, R.; Christy, A.A.; Kumar, A.S.; Mittal, A. Antilion optimization based placement of FACTS devices in power systems Int. J. Pure Appl. Math. **2018**, 118, 333–341.

[21] Nomihla, W.N.; Innocent, E.D.; Katleho, M. Power Planning for a Reliable Southern African Regional Grid. Energies **2023**, 16, 1028.

[22] Farrahi-Moghaddam, F.; Nezamabadi-pour, H.; Malihe, M.F. Curved Space Optimization for Allocation of SVC in a Large Power. In Proceedings of the 6th WSEAS International Conference on Applications of Electrical Engineering, Istanbul, Turkey, 27–29 May 2007.

[23] Pravallika, D.L.; Rao, B.V. Flower Pollination Algorithm based optimal setting of TCSC to minimize the Transmission line losses in the Power System. Procedia Comput. Sci. **2016**, 92, 30–35.

[24] Mishra, A.; Nagesh, V.; Kumar, G. Disparity Line Utilization Factor and Galaxy-Based Search Algorithm for Advanced Congestion Management in Power Systems. Int. J. Technol. **2016**, 1, 88–96.

[25] Sarker, J.; Goswami, S.K. Solution of multiple UPFC placement problems using Gravitational Search

Algorithm. Electr. Power Energy Syst. **2014**, 55, 531–541.

[26] Dharmaraj, K.; Ravi, G. Optimal Location and Setting of FACTS Devices for Reactive Power Compensation Using Harmony Search Algorithm. Automatika **2016**, 57, 881–892.

[27] Devarapalli, R.; Bhattacharyya, B. Power and energy system oscillation damping using multi verse optimization. SN Appl. Sci. **2021**, 3, 383.

[28] Gitizadeh, M.; Kalantar, M. A New Approach for Congestion Management via Optimal Location of FACTS Devices in Deregulated Power Systems. In Proceedings of the 2008 Third International Conference on Electric Utility Deregulation and Restructuring and Power Technologies, Nanjing, China, 6–9 April 2008.

[29] Ghareeb, M.; Mostafa, E.; Ahmed, R.G.; Abdullah, M.S.; Hany, S.E.M. A Gradient-Based Optimizer with a Crossover Operator for Distribution Static VAR Compensator (D-SVC) Sizing and Placement in Electrical Systems. Mathematics **2023**, 11, 1077.

[30] Amin, A.; Ebeed, M.; Nasrat, L.; Aly, M.; Ahmed, E.M.; Mohamed, E.A.; Alnuman, H.H.; Abd El Hamed, A.M. Techno-Economic Evaluation of Optimal Integration of PV Based DG with DSTATCOM Functionality with Solar Irradiance and Loading Variations. Mathematics **2022**, 10, 2543.

[31] Raj, S.; Bhattacharyya, B. Optimal placement of TCSC and SVC for reactive power planning using Whale optimization algorithm. Swarm Evol. Comput. BASE DATA **2017**, 40, 131–143.

[32] Bairu, V.; Kumar, B.V. Power System Loss Minimization by Using UPFC Placed at Optimal Location Given by Artificial Bee Colony Algorithm. Int. J. Res. Advent Technol. **2019**, 7, 127–132.

[33] Dutta, S. Optimal location of STATCOM using chemical reaction optimization for reactive power dispatch problem. Ain Shams Eng. J. **2015**, 7, 233–247.

[34] Choudhary, G.; Singhal, N.; Sajan, K.S. Optimal placement of STATCOM for improving voltage profile and reducing losses using crow search algorithm. In Proceedings of the IEEE International Conference on Control, Computing, Communication and Materials (ICCCCM), Allahabad, India, 21–22 October 2016.

[35] Elshahed, M.; Tolba, M.A.; El-Rifaie, A.M.; Ginidi, A.; Shaheen, A.; Mohamed, S.A. An Artificial Rabbits' Optimization to Allocate PVSTATCOM for Ancillary Service Provision in Distribution Systems. Mathematics **2023**, 11, 339.

[36] Abd-Elazim, S.M.; Ali, E.S. Optimal location of STATCOM in multimachine power system for increasing loadability by Cuckoo Search algorithm. Electr. Power Energy Syst. **2016**, 80, 240–251.

[37] Abubakar, J.; Jibri, Y.; Jimoh, B. Voltage Stability Enhancement by Optimal Sizing and Siting of Static Synchronous Compensator Using Dragonfly Algorithm. Zaria J. Electr. Eng. Technol. **2021**, 10, 47–56.

[38] Selvaganapathy, R.; Kannan, R.; Ravi, A. Allocation of Facts Devices for Power Quality Improvement. Int. J. Electr. Eng. Technol.**2021**, 12, 154–162.

[39] Abdelsalam, A.A.; Mansour, H.S.E. Optimal Allocation and Hourly Scheduling of Capacitor Banks Using Sine Cosine Algorithm for Maximizing Technical and Economic Benefits. Electr. Power Compon. Syst. **2019**, 47, 1025–1039.

[40] Pratap, C.N.; Ramesh, C.P.; Sidhartha, P. Grasshopper optimization algorithm optimized multistage controller for automatic generation control of a power system with FACTS devices. Prot. Control. Mod. Power Syst. **2021**, 6, 8.